A NEW ALGORITHM FOR AUTOMATIC PRECISE RECONSTRUCTION OF A REAL OBJECT SURFACE

Jaan-Rong TSAY*
*National Cheng Kung University, Taiwan, R.O.C.
Institute of Surveying Engineering
tsayjr@mail.ncku.edu.tw

Working Group III/2

KEY WORDS: Reconstruction , Mathematical Models, Algorithms, Automation, DTM/DEM/DSM, Wavelets.

ABSTRACT

This paper proposes some wavelet-based mathematical models and algorithms for representing any 'real' signal such as a 2D curve or a 3D surface. In contrast with conventional methods that describe almost only a smooth approximation, these models are more powerful which can describe effectively not only smooth signals but also multi-resolution fractal ones. By adopting a designed algorithm, they can also resolve the problem caused by *Gibbs effect* so that they still can represent a discontinuous signal accurately. Test results of 2D curves and 3D surfaces are shown and analyzed. Based on those conclusions drawn from experimental tests and theoretical analyses, a new algorithm for automatic reconstruction of a *real* 3D object surface using airborne sensor data (e.g. aerial images) is presented as well. The test results show that high precision representation of a *real* 3D object surface is realizable. Moreover, the proposed wavelet-based algorithm can describe an entire geometrical object surface with local (pseudo) break points and/or –lines, where conventional piecewise representation is not needed.

1 INTRODUCTION

One of the main purposes of surveying engineering is to acquire geometric, physical/radiometric, and semantic data and information about objects of interest. At present, those acquired data and information can be represented in a very user-friendly way, e.g. the so-called 'virtual reality'. In contrast with a conventional analog 2D-map that is not enough user-friendly and loses much object information after map compilation, a 3D virtual reality model is really easy-to-learn because it represents directly a minified real 3D model of surveyed object(s). To make dynamical simulation analysis of interest objects become much more easy and laborsaving, many researches in the field of surveying aim also at automation technologies which utilize multi-sensor, multi-source and/or multi-temporal data and information as well. For instance, an automatic reconstruction of a 3D-object model and thematic information extraction is a hot topic.

This paper presents some preliminary study results. They aim at (semi-) automatic reconstruction of a real 3D-object model, e.g. a so-called 'cybercity' or a 3D sea surface. A 3D object surface can be regarded as a continuous 'signal' of surface height or surface radiometric intensity, where the so-called '*signal*' is generally interpreted as '*a sequence of digital data*' (Meyer and Ryan, 1994). Those real signals such as a geometrical 3D-city surface have almost always the following distinctive properties that traditional methods can not describe exactly or easily:

(1) multi-resolution,
(2) having local surfaces with (pseudo) break points or –lines,
(3) various degree of continuity on different surface points, and
(4) various fractal dimension, where detailed definition of 'fractal dimension' please see (Mandelbrot, 1982; Farge, et. al., 1993).

For example, (pseudo) break points or –lines often can be found on walls right round a building. Blocks of high skyscrapers, blocks of small houses, visible surfaces of separate local trees/forests and some local naked natural earth surface as well compose a multi-resolution city surface with the aforementioned properties.

2 GIBBS EFFECT

2.1 GIBBS Effect

If one wants to represent a (near-) discontinuous signal by using its low-pass filtered approximation, the so-called Gibbs phenomenon (Michelson, 1898; Gibbs, 1899; Carslaw, 1925) will appear. The Gibbs oscillations appear when the highest frequencies of a discontinuous signal are filtered out. Such oscillation effect causes that exact signal representation in the neighboring areas centered at those discontinuous break-lines/points is theoretically impossible. If a signal f with limited energy $\|f\| = \int_{-\infty}^{\infty} |f(x)|^2 dx < \infty$ is discontinuous at $x = x_0$, i.e. $f(x_0^-) \neq f(x_0^+)$, its low-pass filtered approximation f_ξ has the property of (Mallat, 1998)

$$\lim_{\xi \to \infty} \| f - f_\xi \| = 0 \qquad \text{and} \qquad \lim_{\xi \to \infty} | f(x) - f_\xi(x) | \neq 0, \forall x \to x_0 , \tag{1}$$

where ξ is the half band width of the low-pass filter. The error function is

$$f_\xi(x) \quad - \quad f(x) \quad = \quad \{ f(x_0^+) - f(x_0^-) \} u * h_\xi (x - x_0) \qquad \text{for} \qquad \xi \to \infty \tag{2}$$

where $u * h_\xi(t) = h_\xi * u(t) = \int_{-\infty}^{\infty} h_\xi(y) u(t-y) dy$, $u(x) = \begin{cases} 1 & , x \geq 0 \\ 0 & , x < 0 \end{cases}$, and h_ξ is a used low-pass filter. The Gibbs oscillations are created by $u * h_\xi$. For example, figure 1 shows four examples of the function $u * h_\xi$ (t), where different low-pass filters are used. It shows apparently that the influence radius of the Gibbs effect is very large if the ideal low-pass filter $h_\xi(x) = \dfrac{\sin(\xi x)}{\pi x}$ is used. Gibbs oscillations don't appear in the Haar case. The Gibbs effects in the other two cases appear only in a limited local area.

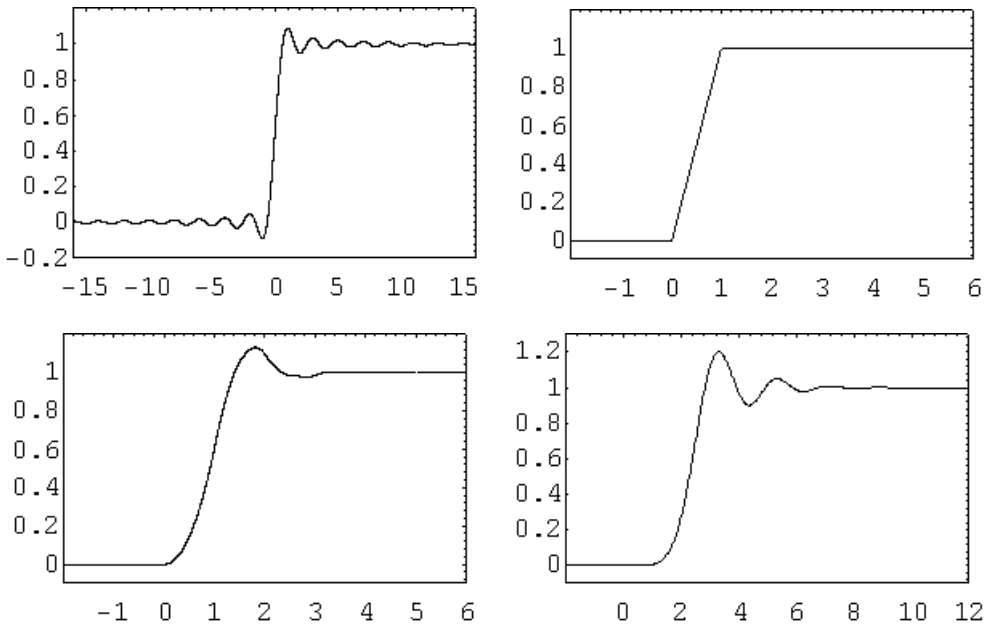

Figure 1. four examples of the function $u * h_\xi$ (t) generated by different h_ξ which is the ideal low-pass filter (upper left), Haar scaling function (upper right), Asymmetric Daubechies scaling function of order N=3 (lower left), and N=10 (lower right), respectively.

Some conclusions are drawn from experimental and theoretical researches that are summarized briefly as follows:

1. The Gibbs effect depends on the Heaviside step function of amplitude $f(x_0^+) - f(x_0^-)$, i.e. $\{ f(x_0^+) - f(x_0^-) \} u(x - x_0)$.

2. The Gibbs effect disappears if the Haar *father wavelet* is used as a basis for low-pass filtering.
3. If $\xi \to \infty$, the over-/under-shoot value of the approximation f_ξ at $x = x_0$ is a constant and about 9% of $|f(x_0^+) - f(x_0^-)|$ for ideal low-pass filter, 4~10% for spline functions (Richards, 1991; Zhang and Martin, 1997), 9% for Fourier series, 0~7% for wavelet series, respectively.
4. If ξ increases, the influence radius decreases. The number of oscillation waves stays constant for all ξ-values. Therefore, Gibbs oscillation becomes a higher frequency wave signal, if ξ increases.

2.2 A SOLUTION FOR APPLICATIONS IN PRACTICE

In practice, a wavelet-based method given by (Tsay, 1999) can be used to solve the Gibbs effect. The method is derived from the fact that all measured data have observation errors and almost all natural or artificial break-lines/points in practice are not exactly theoretical ones. For instance, a wall surface of a building is often not exactly perpendicular to the ground surface. The observation errors and a very small discrepancy of the perpendicular condition for break-lines/points could make the Gibbs effect become very insignificant, if the wavelet-based approximation method is utilized.

3 MATHEMATICAL MODELS FOR REPRESENTING A REAL SIGNAL

After solving the Gibbs problem encountered in practice, the method given by (Tsay, 1999) can be extended using some new wavelet-based mathematical models. They are developed to be able to also represent fractal signals. In fact, the compactly supported orthonormal wavelets of Daubechies display a fractal geometry (Kaiser, 1994).

An approximation of a real signal f with finite energy $\|f\| < \infty$ can be represented by:

$$A_J f = A_{j0} f + \sum_{j=j0}^{J-1} D_j f \qquad \_3\_$$

where

$A_{j0} f = \sum_{k \in z} \alpha_{j0k} \phi_{j0k}$ = an approximation of the signal f with coarser resolution than $A_J f$,

$\alpha_{j0k} = \langle f, \phi_{j0k} \rangle$ = the inner product of f with ϕ_{j0k},

$\phi_{j0k} = \sqrt{2^{j0}} \phi(2^{j0} x - k)$ = a scaling function,

$D_j f = \sum_{k \in z} w_{jk} \psi_{jk}$ = detail component of the signal f,

$w_{jk} = \langle f, \psi_{jk} \rangle$ = the inner product of f with ψ_{jk},

$\psi_{jk} = \sqrt{2^j} \psi(2^j x - k)$ = a wavelet function,

ϕ and ψ are an orthonormal father and mother wavelet function, respectively (Antonini, et. al., 1992; Daubechies, 1994; Meyer and Ryan, 1994).

The 2D-model can be expressed similarly to the equation (1), e.g. see (Mallat, 1998).

In general, such models are based on those orthonormal fractal wavelets that cannot, in general, be written in a closed analytic form. Their graph and the other mathematical computations in practice, such as integration, differentiation, addition, multiplication, division, etc., can be computed with arbitrarily high precision by some specified methods, please see (Tsay, 1996).

4 TEST RESULTS AND ANALYSIS

4.1 Representation of A 2D Curve

The so-called 'wavelet series (=WS)' as shown in the equation (3) can be used to represent a 2D curve. For example, figure 2 shows a 'house' profile line and its WS-represented profile line with J=7. The upper right part of the 'house' profile line is also compared with its WS-represented curves with J=1, 3, and 7, where the compactly supported orthonormal asymmetric Daubechies wavelets of order N=3 is used. Here, the line is represented as $x(l_i)$ and $y(l_i)$, where l_i is the path length from a chosen start point to the i-th point along the line, (x,y) is the coordinates of this i-th point. Both functions $x(l_i)$ and $y(l_i)$ can be represented using the WS. Apparently, the finer the resolution used in the WS, the more accurate the represented curve. Furthermore, the Gibbs effect can be effectively reduced or completely disappear so that an accurate representation of a discontinuous curve (or line) is applicable.

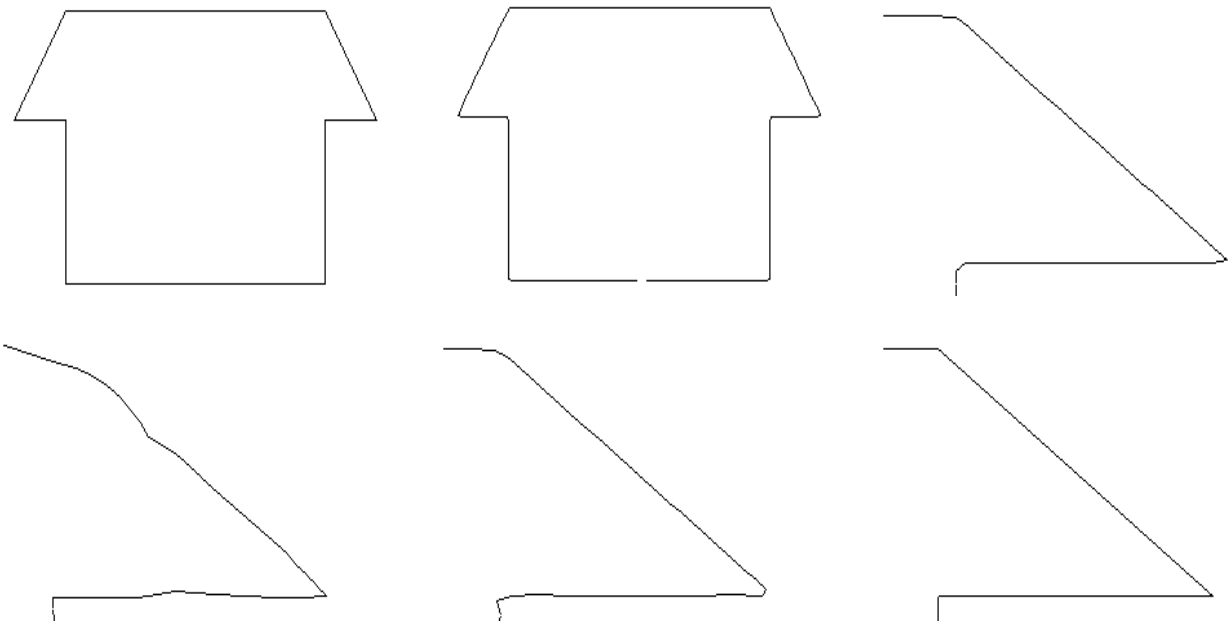

Figure 2. a 'house' profile line (upper left), WS-represented profile line with J=7 (upper middle), upper right part of the 'house' profile line (upper right), WS-represented curves of the upper right part of the 'house' profile line with J=1 (lower left), J=3 (lower middle), and J=7 (lower right), where asymmetric Daubechies wavelets of order N=3 is used.

For theoretical analysis, different types of simulated signals f such as city profile functions, city surface functions, step functions and so on, are used as test data. In all tests, each f is known. Therefore, one can determine the true error of $A_J f$ and analyze its convergence characteristics. The conclusions will be given briefly as follows.

The algorithm for wavelet-based representation is most effective and efficient, if a from-coarse-to-fine strategy is used to determine the locations of significant wavelet coefficients. The accuracy of such an approximation becomes better if a finer resolution (i.e. a larger J-value) is adopted, where J is a resolution index. The influence radius of the Gibbs phenomenon becomes smaller in a rate of 2^{-J} as the J-value becomes larger. The ratio of the maximal approximation error near a pseudo break point to the signal height difference at that break point is a constant. On the other hand, the Daubechies wavelet of 3rd order is the best basis comparing to the other representative bases such as the Haar wavelet, the Meyer wavelet and the Fourier basis. It is also very suitable to describe different kinds of signals, e.g. a smooth signal, a rugged one and a signal with local break points.

4.2 Representation of A Real 3D-City Surface

The applicability analyses of the proposed mathematical models and algorithms are also done using a real geometrical city model in a suburb of Taipei. The model is measured on analytical plotter Leica BC3 using a stereo pair of aerial photos with a mean photo scale 1/5000, photo format 23cm x 23cm, and focal length 30cm. The analog photos are scanned using photo scanner DSW200 with a pixel size of 25 µm x 25µm. The measured 3D points in the stereo model are then edited to produce a geometrical surface in the test area shown in Figure 3.

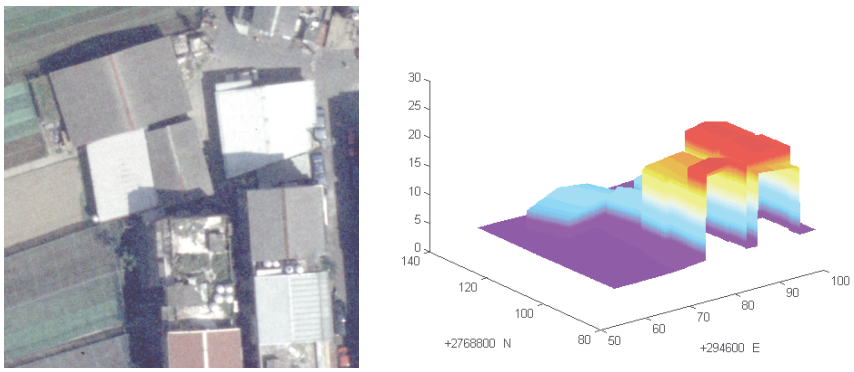

Figure 3. Aerial image in test area (left) and geometrical surface of the test area (right)

The geometrical surface is taken as a known real 3D-city surface that is used to examine the accuracy and characteristics of the wavelets-based approximation algorithm. Some test results are shown in Figures 4. Apparently, approximation function $A_J f$ can converge to f as the resolution becomes finer, namely the index J becomes larger.

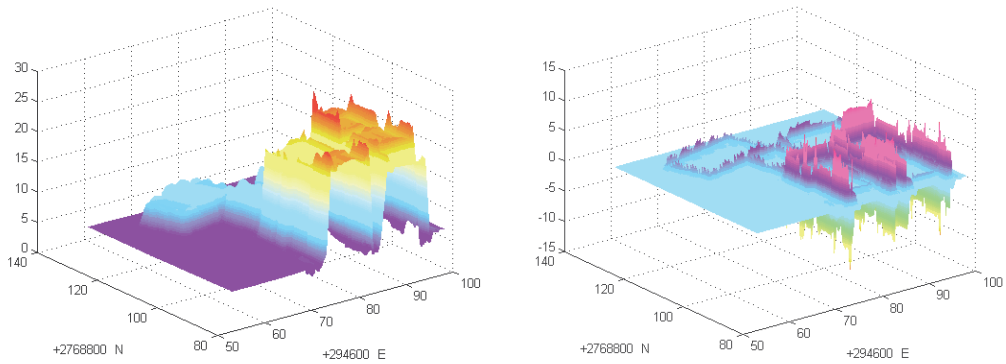

(a) Approximation $A_0 f$ (left) and its error function (right)

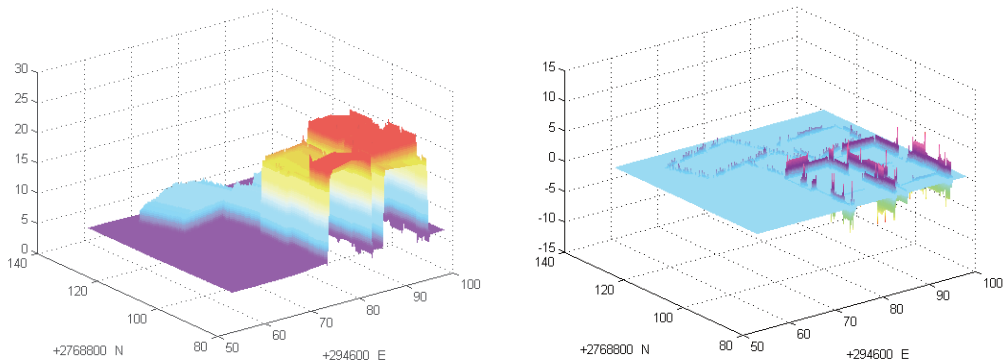

(b) Approximation $A_2 f$ (left) and its error function (right)

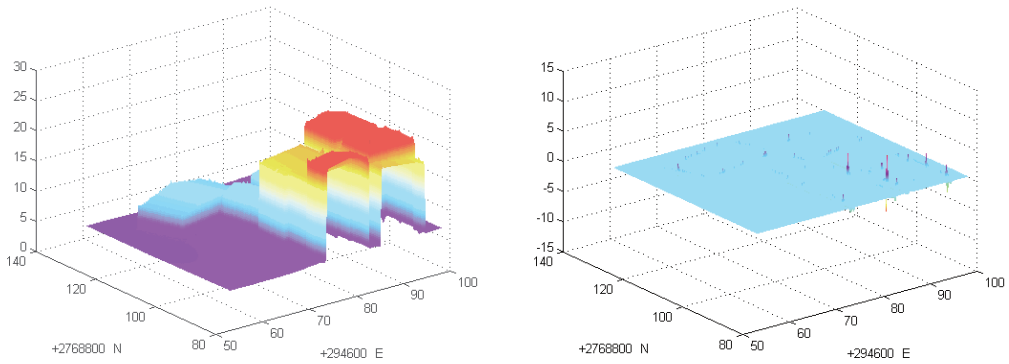

(c) Approximation $A_4 f$ (left) and its error function (right)

Figure 4. Approximations $A_j f$ and their error functions with j = 0, 2, 4

In addition, one can superimpose the digital image data on the computed geometrical surface and get a virtual reality of the 3D-city surface in test area as shown in figure 5. The image information on all walls is evidently insufficient because only aerial images are used in these tests. Moreover, a dynamical stereoscopic view can also be done, if the related computer hardware and software are available. It is really an easy-to-learn and user-friendly 3D 'map'.

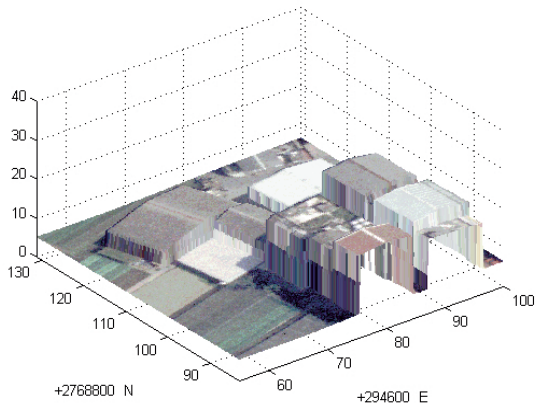

Figure 5. Virtual reality of the 3D-city surface in test area

5 A CONCEPT FOR AUTOMATIC RECONSTRUCTION OF A REAL 3D OBJECT SURFACE

The main concept to do automatic and high precision reconstruction and analysis of a real 3D object surface having the in section 1 described properties (1)_(4) is drawn from the method of *facets stereo vision* (Tsay, 1998). Orthonormal fractal wavelets such as the compactly supported Daubechies wavelets (Daubechies, 1992) are used to define a feasible functional model in the object space to describe a real geometric and/or radiometric object surface. Moreover, the principles of 'image inversion', 'sampling theorem' and 'least squares estimation technique' are applied together with the 'from-coarse-to-fine' strategy. It is a method for automatic generation of a digital terrain model and an ortho image, where digital images are the basic observations. It can also integrate in principle multi-sensor and multi-source data to provide reliable and accurate results for photogrammetry and remote sensing. The first draft of facets stereo vision was proposed publicly in 1987 (Wrobel, 1987).

The concept would further extend and improve the method of (Tsay, 1998) with the new capability for representing a real signal with the aforementioned properties (1)~(4). More explicitly to say, the idea aims for an automatic *image inversion method* to get object information. The method must be able to represent *fractal geometry*. For the present, only fractal geometry can correctly describe and analyze real natural objects. Therefore, fractal geometry is apparently the *correct mathematics* (Jaehne, 1991).

For the purpose stated in section 1, a thorough research of models and algorithms for representing a signal having the properties (1)_(4) is done. Some known simulated and representative 2D signals, chiefly 2D-city profile functions, and a 3D-city surface function are used to do the van study, especially about the characteristics and accuracy of the proposed algorithm for representing the above-mentioned signals.

In accordance with those conclusions, a first draft of an algorithm for automatic reconstruction of a real 3D object surface is depicted briefly in Figure 6. It adopts the above-mentioned concept, i.e. orthonormal fractal wavelets, the principles of image inversion, sampling theorem, least squares estimation technique, and a 'from-coarse-to-fine' strategy are utilized. In each level of the image pyramid, significant wavelet coefficients are automatically determined and selected and used as candidate unknown parameters for the lower level with finer resolution, so that an efficient operations are available.

Compute the image pyramid data.
Define approximation of DTM: horizontal plane or better data if available.
Compute a better DTM by the image pyramid method:
From the top to the bottom level:
For the top level:
Determine α_{j0k} and w_{j0k}, $\forall k$.
Automatically select significant wavelet coefficients w_{j0k}, $\forall k$.
Prolong the significant wavelet coefficients to the lower level.
For the lower levels:
Determine w_{jk} for those candidates of significant wavelet coefficients.
Automatically select significant wavelet coefficients w_{jk}, $\forall k$.
Prolong the significant wavelet coefficients to the lower level.
For the bottom level:
Determine w_{jk} for those candidates of significant wavelet coefficients.
Automatically select significant wavelet coefficients w_{jk}, $\forall k$.
Output the computed DTM and ortho image and its covariance matrix as well.

Figure 6. First draft of an algorithm for automatic reconstruction of a real 3D-city surface

6 CONCLUSIONS

1. If the half band width of the used low-pass filter increases, i.e. $\xi \to \infty$, the over-/under-shoot value of the approximation f_ξ at discontinuous point $x = x_0$ is a constant and about 9% of $| f(x_0^+) - f(x_0^-) |$ for ideal low-pass filter, 4~10% for spline functions, 9% for Fourier series, 0~7% for wavelet series, respectively.

2. The algorithm is most effective and efficient, if a from-coarse-to-fine strategy is used to determine the locations of significant wavelet coefficients. The accuracy of such an approximation becomes better if a finer resolution (i.e. a larger j-value) is adopted. The influence radius of the Gibbs phenomenon becomes smaller in a rate of 2^{-J} as the *J*-value becomes larger, where *J* is a resolution index. The ratio of the maximal approximation error near a pseudo break point to the signal height difference at that break point is a constant. On the other hand, the Daubechies wavelet of 3rd order is the best basis comparing to the other representative bases, namely the Haar wavelet, the Meyer wavelet and the Fourier basis. It is very suitable to describe different kinds of signals, e.g. a smooth signal, a rugged one and a signal with local break points.

3. The state-of-the-art computer science and technology causes a revolutionary progress on the representation form of surveyed object(s), namely from a conventional 2D-map to an easy-to-learn 3D virtual reality of surveyed object(s).

4. The proposed wavelet-based approximation algorithm can describe an entire geometrical function with local (pseudo) break points and/or –lines, where conventional piecewise representation is not needed.

Some topics must be further and continuously studied, e.g. the first draft of algorithm shown in Figure 6 will be exactly developed and tested. Furthermore, a really 3D representation will be further studied, where one changes the current

model Z(X,Y) with only one Z-value at a horizontal position (X,Y) to the other with the capability for representing more Z-values at a (X,Y).

ACKNOWLEDGMENTS

I am most grateful to the National Science Council, Taiwan, R.O.C. that supported this work.

REFERNENCES

Antonini, M., Barlaud, M., Mathieu, P., Daubechies, I., 1992. Image Coding Using Wavelet Transform. IEEE Transactions on Image Processing, Vol. 1, No. 2., pp. 205-220.

Carslaw, H.S., 1925, A Historical Note on Gibbs phenomenon. Bull. Amer. Math. Soc., 31, pp. 420-424.

Daubechies, I., 1992. Ten Lectures on Wavelets. Society for Industrial and Applied Mathematics, Philadelphia, Pennsylvania, pp. 194-202.

Farge, M., Hunt, J.C.R., and Vassilicos, J.C., 1993. Wavelets, Fractals and Fourier Transforms. Clarendon Press.

Gibbs, J.W., 1899, Letter to the editor, Nature 59, page 606.

Jaehne, B., 1991. Digitale Bildverarbeitung. 2nd edition, Springer Verlag.

Mallat, S., 1998. A Wavelet Tour of Signal Processing. Academic Press.

Mandelbrot, B., 1982. The Fractal Geometry of Nature. San Francisco: Freeman.

Meyer, Y., and Ryan, R.D., 1994. Wavelets – Algorithms & Applications. 2nd printing, Society for Industrial and Applied Mathematics, Philadelphia, Pennsylvania.

Michelson, A.A., 1898, Letter to the editor, Nature 58, pp. 544-545.

Kaiser, G., 1994. A Friendly Guide to Wavelets. Birkhaeuser, pp. 183-189.

Richard, F.B., 1991. A Gibbs phenomenon for spline functions. Journal of Approximation Theory 66, pp.344-351.

Tsay, J.R., 1996. Wavelets fuer das Facetten-Stereosehen. Deutsche Geodaetische Kommission, Reihe C, Dissertation, Heft Nr. 454, Munich, Germany, pp. 66-74.

Tsay, J.R., 1998. A New Algorithm for Surface Determination Based on Wavelets and its Practical Application. Photogrammetric Engineering & Remote Sensing, Vol. 64, No. 12, pp. 1179-1188.

Tsay, J.R., 1999, A wavelet-based method to solve the Gibbs problem in practice. Journal of the Chinese Institute of Civil and Hydraulic Engineering, Vol. 11, No. 3, pp. 543-550.

Wrobel, B.P., 1987. Digital Image Matching by Facets Using Object Space Models, SPIE (=The International Society for Optical Engineering), 804, pp. 325-333.

Zhang, Z., and Martin, C.F., 1997. Convergence and Gibbs' phenomenon in cubic spline interpolation of discontinuous functions, Journal of Computational and Applied Mathematics 87, pp. 359-371.